The EMBO Journal vol.15 no.9 pp.2056–2068, 1996

Implications for the domain arrangement of axonin-1 derived from the mapping of its NgCAM binding site

Christoph Rader, Beat Kunz, Ruth Lierheimer, Roman J.Giger, Philipp Berger, Peter Tittmann[1], Heinz Gross[1] and Peter Sonderegger[2]

Institute of Biochemistry, University of Zurich, CH-8057 Zurich and [1]Institute of Cell Biology, ETH Zurich, CH-8093 Zurich, Switzerland

[2]Corresponding author

The neuronal cell adhesion molecule axonin-1 is composed of six immunoglobulin and four fibronectin type III domains. Axonin-1 promotes neurite outgrowth, when presented as a substratum for neurons *in vitro*, via a neuronal receptor that has been identified as the neuron–glia cell adhesion molecule, NgCAM, based on the blocking effect of polyclonal antibodies directed to NgCAM. Here we report the identification of axonin-1 domains involved in NgCAM binding. NgCAM-conjugated microspheres were tested for binding to COS cells expressing domain deletion mutants of axonin-1. In addition, monoclonal antibodies directed to axonin-1 were assessed for their ability to block the axonin-1–NgCAM interaction, and their epitopes were mapped using the domain deletion mutants. The results suggest that the four amino-terminal immunoglobulin domains of axonin-1 form a domain conglomerate which is necessary and sufficient for NgCAM binding. Surprisingly, NgCAM binding to membrane-bound axonin-1 was increased strongly by deletion of the fifth or sixth immunoglobulin domains of axonin-1. Based on these results and on negative staining electron microscopy, we propose a horseshoe-shaped domain arrangement of axonin-1 that obscures the NgCAM binding site. Neurite outgrowth studies with truncated forms of axonin-1 show that axonin-1 is a neurite outgrowth-promoting substratum in the absence of the NgCAM binding site.

Keywords: axonin-1/domain arrangement/immunoglobulin superfamily/neuronal cell adhesion molecules/NgCAM

Introduction

The formation of a complex network of neurons during the development of the nervous system is based on specific interactions amongst neurons and between neurons and their environment. These interactions are likely to be mediated by surface glycoproteins present on the axons' leading tip, the growth cone, acting as specific recognition molecules to guide axons to their targets (Patterson, 1992; Goodman and Shatz, 1993). Among the presently known molecules considered to be involved in axon guidance, neural surface glycoproteins of the immunoglobulin (Ig) superfamily play a prominent role. These have been categorized into molecules composed of Ig domains only or of Ig domains in conjunction with fibronectin type III (FNIII) domains (Rathjen and Jessell, 1991). Based on structural criteria, i.e. membrane anchorage and particular combinations of Ig and FNIII domains, the family of Ig/FNIII neural glycoproteins can be divided further into several subgroups (Vielmetter *et al.*, 1994). The glycosylphosphatidylinositol (GPI)-anchored proteins contactin/F11/F3, TAG-1/axonin-1, PANG/BIG-1 and BIG-2 constitute one such subgroup and are striking particularly in their spatially and temporally restricted patterns of expression during neuronal development (Ranscht, 1988; Brümmendorf *et al.*, 1989; Gennarini *et al.*, 1989; Furley *et al.*, 1990; Zuellig *et al.*, 1992; Connelly *et al.*, 1994; Yoshihara *et al.*, 1994, 1995). They are composed of six Ig and four FNIII domains separated by a glycine/proline-rich segment. Their modular assembly suggests that the GPI-anchored Ig/FNIII neural glycoproteins regulate axonal elongation along specific pathways by multiple macromolecular interactions (Sonderegger and Rathjen, 1992), and, indeed, several specific binding activities have now been demonstrated *in vitro* (Brümmendorf and Rathjen, 1993). Axonin-1 of the chick has been shown to bind homophilically (Rader *et al.*, 1993) and heterophilically to neuron–glia cell adhesion molecule (NgCAM; Kuhn *et al.*, 1991) and Ng-CAM-related cell adhesion molecule (NrCAM/Bravo; Suter *et al.*, 1995). Both NgCAM and NrCAM/Bravo belong to a subgroup of Ig/FNIII neural glycoproteins which are composed of six Ig and five FNIII domains, a single transmembrane segment and a cytoplasmic tail (Burgoon *et al.*, 1991; Grumet *et al.*, 1991; Kayyem *et al.*, 1992). The recent description of axonin-1, NgCAM and NrCAM/Bravo as the molecules involved in the pathfinding decision of spinal commissural axons at the floor plate (Stoeckli and Landmesser, 1995) puts these molecules in the focus of current interest as one of the best described pathfinding models in vertebrates.

The interaction of axonin-1 and NgCAM was concluded to mediate the promotion of neurite outgrowth of chicken embryonic dorsal root ganglion neurons on axonin-1 substratum *in vitro*, as evidenced by the virtually complete arrest of neurite outgrowth in the presence of polyclonal antibodies directed to NgCAM (Kuhn *et al.*, 1991). To understand better the functional implications of this interaction, we have begun a detailed structure/function analysis of axonin-1–NgCAM binding. Here we report the identification of the NgCAM binding site on axonin-1 and propose a model for the domain arrangement of axonin-1. With this structure, membrane-bound axonin-1 may interact with NgCAM of the same membrane rather than with NgCAM of an apposed membrane. Thus, it is unlikely that NgCAM is the growth cone receptor for neurite outgrowth on axonin-1 substratum. Neurite outgrowth studies support this prediction.

Results

The deletion of the fifth and the sixth Ig domain of axonin-1 results in an increased binding of NgCAM

Entire domains of axonin-1, as defined by their homology to the Ig constant domains or the type III domains of fibronectin (Zuellig *et al.*, 1992) and by exon–intron borders of the axonin-1 gene (Giger *et al.*, 1995), were deleted by oligonucleotide-directed mutagenesis and cloned into the axonin-1 expression vector pSCT-axonin-1. Vectors carrying these constructs were introduced into COS cells by electroporation. The transiently transfected cells were solubilized 2 days after transfection, and analysed for axonin-1 expression by immunoblotting. The sizes of the axonin-1 domain deletion mutants were in agreement with the predicted values (Figure 1). No axonin-1 immunoreactivity was detectable on parental COS cells. Immunofluorescence analyses revealed that all mutants, except the one where the most amino-terminal Ig domain was deleted, designated ΔIg1, were expressed on the surface of COS cells in similar quantities to wild-type axonin-1 (data not shown). ΔIg1, although apparently absent from the cell surface, was detected in similar quantities to wild-type axonin-1 when solubilized membranes were analysed by immunoblotting (Figure 1A), suggesting that ΔIg1 was produced but remained inside the cell. Treatment with phosphatidylinositol-specific phospholipase C revealed a GPI anchorage of axonin-1 heterologously expressed by COS cells (data not shown). Usually 20–30% of the cells expressed heterologous protein after transfection by electroporation. Two days after transfection, cells were incubated with NgCAM-conjugated polystyrene microspheres (Covaspheres) and, after washing and fixation, axonin-1-expressing cells were identified by indirect immunofluorescence staining. An initial series of axonin-1 domain deletion mutants included the complete set of single domain deletions and three double domain deletions in the amino-proximal region (Figure 2A). The NgCAM binding properties of these mutants together with wild-type axonin-1 are summarized in Figure 2B. Surprisingly, wild-type axonin-1 expressed on the surface of COS cells was found to bind NgCAM-conjugated Covaspheres only weakly. The same result was obtained with wild-type axonin-1 heterologously expressed on the surface of myeloma and fibroblasts cell lines (data not shown), and was in striking contrast to the results of Covaspheres aggregation assays where a strong interaction of native or recombinant axonin-1 and NgCAM had been detected with both binding partners covalently coupled to Covaspheres (Kuhn *et al.*, 1991; Rader *et al.*, 1993). These findings suggested that the failure of recombinant membrane-bound axonin-1 to interact with NgCAM may not be ascribed to its heterologous expression but, probably, to a difference in the accessibility of the NgCAM binding site of axonin-1 when covalently coupled to Covaspheres compared with when membrane-bound. The NgCAM binding properties of the axonin-1 domain deletion mutants supported this view. Whereas cells expressing ΔIg12, ΔIg2, ΔIg23, ΔIg3, ΔIg34, ΔIg4, ΔFn2 and ΔFn3 did not bind NgCAM-conjugated Covaspheres, transfectants expressing ΔIg5 and ΔIg6 exhibited a strongly increased NgCAM binding when compared with cells transfected with wild-type axonin-1 (Figure 2B). To a lesser degree,

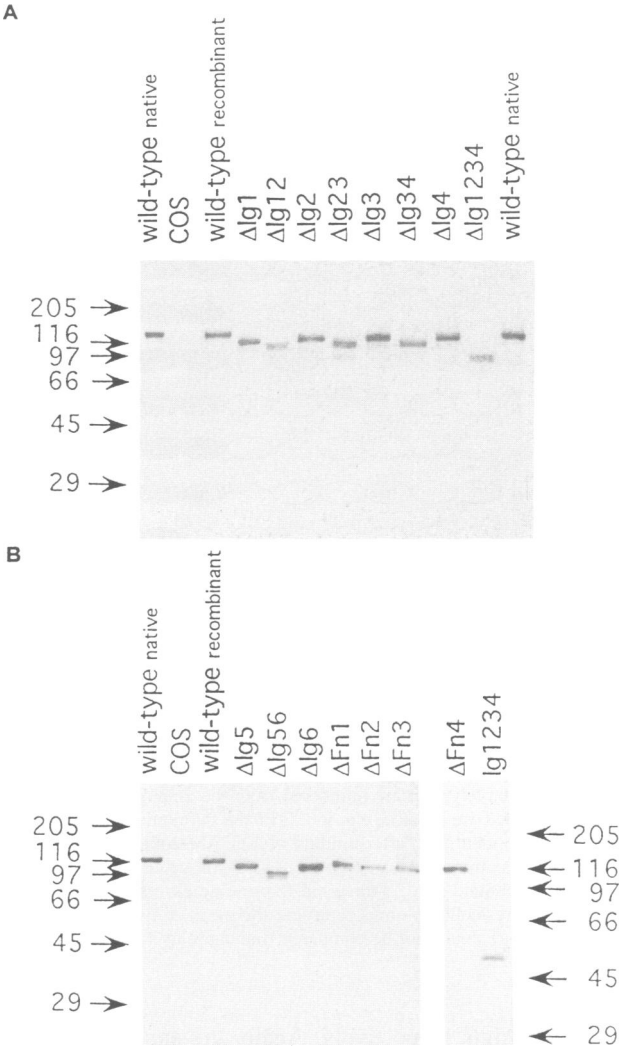

Fig. 1. Size analysis of wild-type axonin-1 and axonin-1 domain deletion mutants of transiently transfected COS cells. Solubilized membranes of non-transfected COS cells ('COS') and COS cells transfected with wild-type axonin-1 ('wild-type recombinant') or domain deletion mutants of axonin-1 (for labels see Figure 2) were subjected to SDS–PAGE (7.5%), electrotransferred to nitrocellulose and immunostained with a mixture of four anti-axonin-1 mAbs followed by peroxidase-conjugated secondary antibodies. The epitopes of the four mAbs used for immunostaining had been mapped to sites beyond (**A**) or within (**B**) the four amino-terminal Ig domains of axonin-1. Vitreous fluid of 14-day-old chicken embryos ('wild-type native') was blotted for comparison. Numbers on the edge indicate the molecular masses of marker proteins in kDa.

ΔFn4 also was found to exhibit increased NgCAM binding. No difference between ΔFn1 and wild-type axonin-1 was detected. These results suggest that the presence of Ig5 and Ig6 in axonin-1 somehow masks the NgCAM binding site of membrane-bound axonin-1.

The four amino-terminal Ig domains of axonin-1 are necessary and sufficient for NgCAM binding

To localize the NgCAM binding site we exploited the apparent unmasking of this site exhibited by Ig5 and Ig6 deletion mutants. In a second series of domain deletion mutants (Figure 3A), double domain deletions were constructed by combining each single domain deletion with

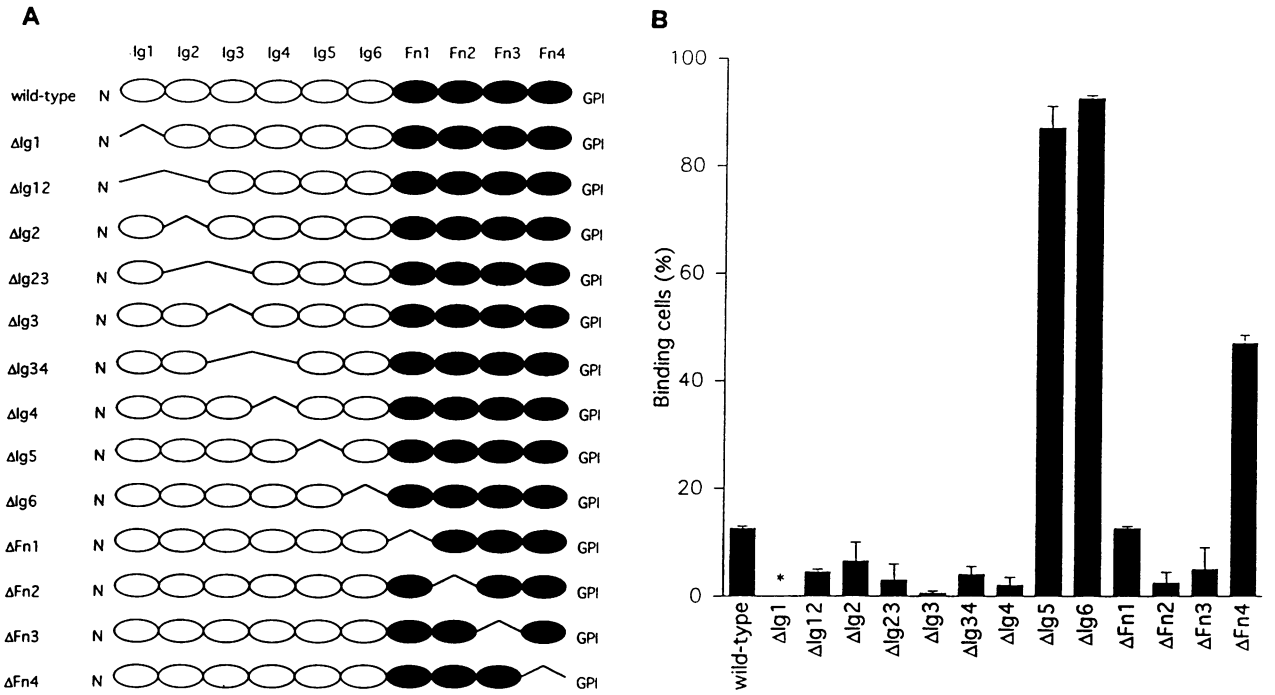

Fig. 2. NgCAM binding by wild-type axonin-1 and the initial series of axonin-1 domain deletion mutants. (**A**) The initial series of axonin-1 domain deletion mutants. Coding regions of wild-type axonin-1 and domain deletion mutants are drawn schematically. Amino-termini are on the left ('N'), and carboxy-termini with post-translationally attached GPI anchors are on the right ('GPI'). Ig and FNIII domains are presented as open and solid ellipses, respectively, and are numbered from the amino- to the carboxy-terminus. Lines indicate domain deletions. The names of mutants indicate the domains that are deleted, e.g. in ΔIg12 the two amino-terminal domains of axonin-1 were excised. (**B**) COS cells expressing wild-type or mutant axonin-1 were identified, after binding of NgCAM-conjugated TRITC Covaspheres and fixation, by indirect immunofluorescence using polyclonal antibodies to axonin-1 and a secondary FITC-conjugated antibody. For each mutant, 100 green fluorescing cells were analysed. Green fluorescing cells that had bound at least three red fluorescing Covaspheres were scored as binding cells. The analysis of unstained cells revealed a background of 0.1 Covaspheres/cell. Columns represent the mean of two independent experiments (error bars indicate SD). Because of its low surface expression, the mutant ΔIg1 could not be compared (indicated by *). Note the increased NgCAM binding of mutants ΔIg5, ΔIg6 and ΔFn4 compared with wild-type axonin-1.

ΔIg5 and ΔIg6, respectively. Again, the expression level of all mutants except the low-expressing ΔIg51 and ΔIg61 transfectants was found to be similar to wild-type axonin-1 (data not shown). The NgCAM binding properties of the second series of axonin-1 mutants are summarized in Figure 3B. Loss of NgCAM binding was detected when ΔIg2, ΔIg3 or ΔIg4 were combined with ΔIg5 or ΔIg6. Although surface expression was low in most cells, a small percentage of ΔIg51 and ΔIg61 transfectants were found to have a comparable expression level. These cells also did not bind NgCAM Covaspheres. In striking contrast, all combinations of ΔIg5 and ΔIg6 with deletions of the FNIII domains were found to exhibit NgCAM binding as strong as ΔIg5 and ΔIg6 alone. Likewise, the double deletion of Ig5 and Ig6, designated ΔIg56, showed no difference in NgCAM binding compared with the single deletions. These results strongly suggest that the NgCAM binding site resides in the four amino-terminal Ig domains of axonin-1. For confirmation, two additional axonin-1 mutants were constructed (Figure 4). Ig1234 coupled the four amino-terminal Ig domains directly to the GPI anchor, and ΔIg1234 was complementary in having these same four domains deleted. Whereas no NgCAM binding was found in the case of ΔIg1234, Ig1234 exhibited strong binding in the same range as ΔIg5 and ΔIg6 (Figure 4). This finding demonstrated the four amino-terminal Ig domains of axonin-1 to be sufficient for NgCAM binding. In addition, it implies that the entirety of these domains is necessary for NgCAM binding: As shown in Figure 3B, all domain deletions involving Ig1, Ig2, Ig3 and Ig4 resulted in a complete loss of NgCAM binding. For further confirmation, single domains of the axonin-1 mutant Ig1234 were excised. The resulting mutants, designated Ig234, Ig134, Ig124 and Ig123, were found to have lost the NgCAM binding property of Ig1234 completely (data not shown). Clearly, the four amino-terminal Ig domains of axonin-1 were found to be necessary and sufficient for NgCAM binding.

The NgCAM binding properties of axonin-1 suggest a backfolded shape which is supported by electron microscopy

The finding that the four amino-terminal Ig domains directly coupled to the GPI anchor exhibit markedly increased NgCAM binding as compared with wild-type axonin-1 (Figures 2 and 4) supports the suggestion that the presence of Ig5 and Ig6 masks the NgCAM binding site. This feature of membrane-bound axonin-1 could be explained by a backfolded shape: the amino-terminal NgCAM binding site folds back towards the membrane and becomes masked by parts of the axonin-1 structure beyond the four amino-terminal Ig domains, namely Ig5 and Ig6. The predicted overall shape of axonin-1 was confirmed by electron microscopy of native axonin-1 molecules (Figure 5). Electron micrographs of negatively stained axonin-1 molecules showed exclusively horseshoe-

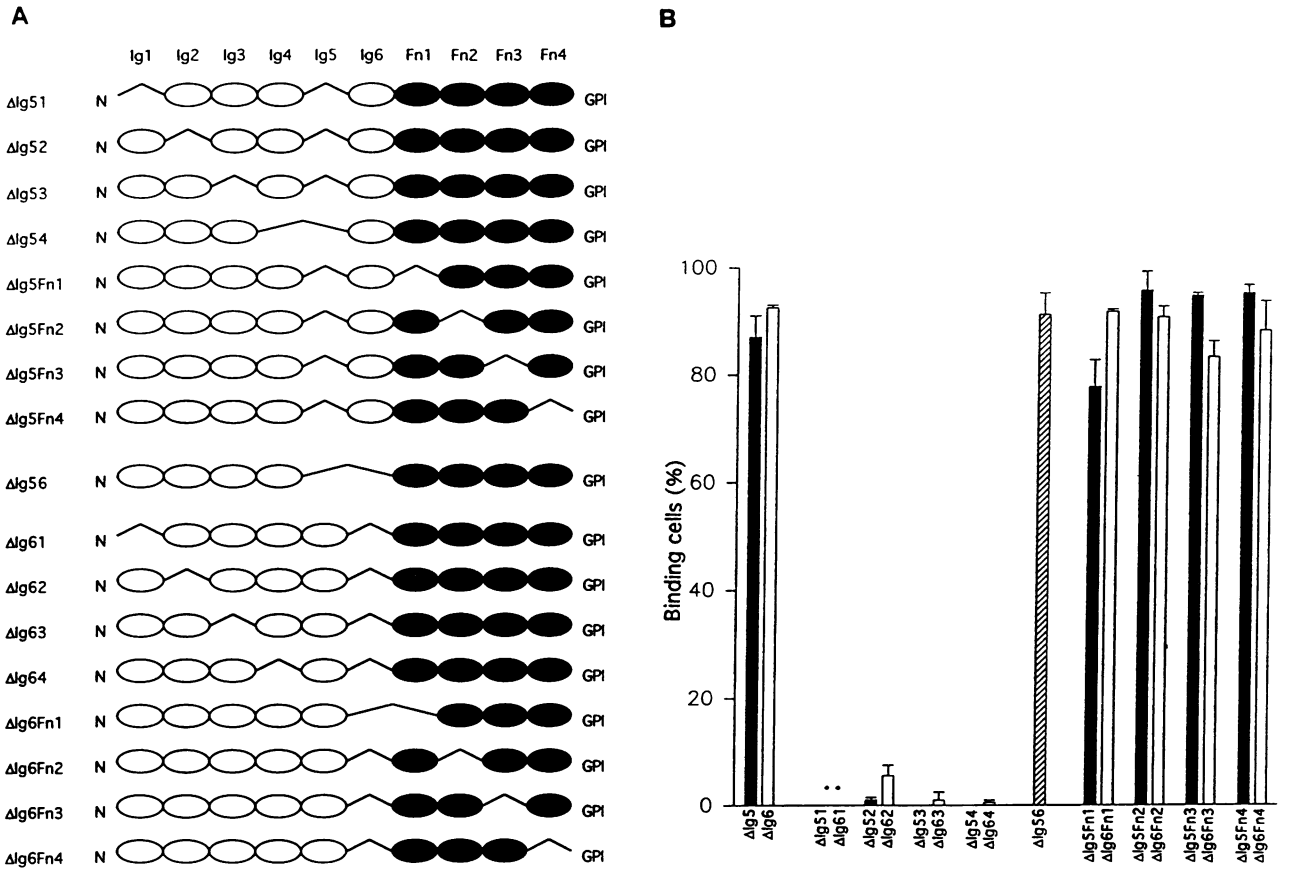

Fig. 3. NgCAM binding by the second series of axonin-1 domain deletion mutants. (**A**) Double domain deletions were constructed by combining each single domain deletion outlined in Figure 2 with ΔIg5 and ΔIg6, respectively. For symbols and labels see Figure 2. (**B**) The Covaspheres binding assay was performed and evaluated as described for Figure 2. Solid and open columns refer to double domain deletions on the basis of ΔIg5 and ΔIg6, respectively; the hatched column refers to the double domain deletion ΔIg56. Columns represent the mean of two independent experiments (error bars indicate SD). Because of their low surface expression, mutants ΔIg51 and ΔIg61 were not taken into consideration (indicated by *); however, no NgCAM binding was detected in the small percentage of cells with a comparable expression level.

shaped structures, the uniform appearance suggesting little segmental flexibility. The size of each arm of the horseshoe was ~10×4 nm and the distance between the arms was ~5 nm (data not shown). As known from crystallographic data, the dimensions of a single Ig or FNIII domain are ~4×2.5×2 nm (Amzel and Poljak, 1979; Leahy *et al.*, 1992). Thus, the size of the horseshoe-shaped structures is large enough to comprise the 10 modules of one axonin-1 molecule, but too small to allow the interpretation of these structures as axonin-1 dimers. In addition, we proved by sedimentation equilibrium ultracentrifugation that soluble axonin-1 molecules do not form aggregates below a concentration of 10 mg/ml (data not shown), while the electron microscopy data are based on an axonin-1 concentration of 75 μg/ml. The horseshoe-shaped structure of axonin-1 as revealed by electron microscopy is in good agreement with the backfolded shape proposed on the basis of the NgCAM binding properties of the axonin-1 domain deletion mutants.

The four amino-terminal domains of axonin-1 form a domain conglomerate

The whole of the four amino-terminal Ig domains was found to be required for NgCAM binding. As a result, deletion analyses within this region do not allow the localization of the actual binding site. To obtain independent data to extend this mapping analysis, a selection of 13 monoclonal antibodies (mAbs) directed to axonin-1 was included in the binding assays. Based on axonin-1 deletion mutants and indirect immunofluorescence analyses, eight mAbs, namely V3B3, X7F6, X7H5, X3G12, X7G9, V9H6, X9C12 and X9H8, had been mapped to the four amino-terminal Ig domains (Table I). The epitopes of the remaining five mAbs V1F1, X9A11, X9B10, X9A9 and X9C3 were localized to domains Ig5, Fn1, Fn2, Fn3 and Fn4, respectively (data not shown). Control experiments had revealed that none of the selected mAbs binds NgCAM. The interference of the mAbs with binding of NgCAM-conjugated Covaspheres to membrane-bound axonin-1 was investigated based on COS transfectants transiently expressing the axonin-1 mutant ΔIg6 (Figure 6A). Two out of 13 mAbs, namely X9H8 and X7F6, were found to interfere strongly with NgCAM binding. Both mAbs had been mapped to the four amino-terminal Ig domains. In contrast, none of the tested mAbs with epitopes beyond Ig1–Ig4 influenced NgCAM binding. This finding confirmed that the NgCAM binding site of axonin-1 resides in the four amino-terminal Ig domains. Figure 6B shows that mAb X9H8 interfered as strongly with the binding of NgCAM Covaspheres by cells expressing the axonin-1 mutant ΔIg6 as polyclonal antibodies raised against axonin-1. In addition, X9H8 also

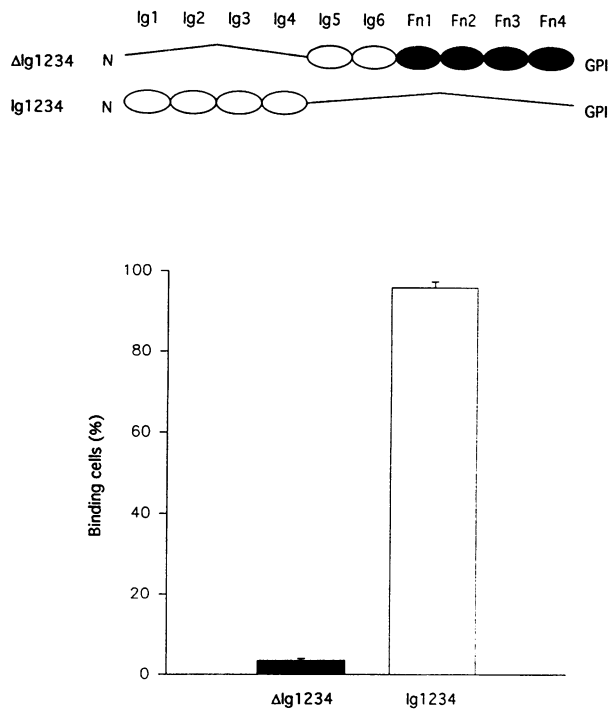

Fig. 4. NgCAM binding by the complementary axonin-1 mutants ΔIg1234 and Ig1234. For symbols, labels and quantitative analysis see Figure 2. The solid column indicates NgCAM binding by ΔIg1234, the open column that of Ig1234. Columns represent the mean of two independent experiments (error bars indicate SD).

prevented the interaction of NgCAM with wild-type axonin-1 and the axonin-1 mutant Ig1234, respectively (Figures 6B and 7). This indicates that the axonin-1 mutants with increased NgCAM binding expose the same NgCAM binding site as that in wild-type axonin-1.

To narrow down further the NgCAM binding site, epitopes of the eight mAbs that had been mapped to the four amino-terminal Ig domains were analysed in more detail. Table I shows that only four out of eight epitopes could be localized to a single domain, either Ig1 or Ig4. One mAb, X7H5, required the presence of two domains, Ig1 and Ig4, for binding, and mAb X3G12, mapped to Ig4, exhibited diminished binding on mutants with a deletion of Ig1, suggesting a close physical association of Ig1 and Ig4. The entirety of all four amino-terminal domains was found to be necessary for the binding of three mAbs, a binding property strongly resembling that of NgCAM reported before. The mAb X9H8, found to interfere with NgCAM binding most potently, belongs to this latter group. From these data we conclude that a close physical association of the four amino-terminal Ig domains exists and that binding of NgCAM requires the whole of this conglomerate.

The NgCAM binding site of axonin-1 is not necessary for neurite outgrowth on axonin-1 substratum in vitro

Axonin-1 adsorbed to tissue culture plastic was found to promote neurite outgrowth of cultured embryonic dorsal root ganglion neurons (Stoeckli *et al.*, 1991). The growth cone receptor for adsorbed axonin-1 was concluded to be NgCAM, based on the fact that neurite outgrowth on axonin-1 was blocked by NgCAM antiserum Fab (Kuhn

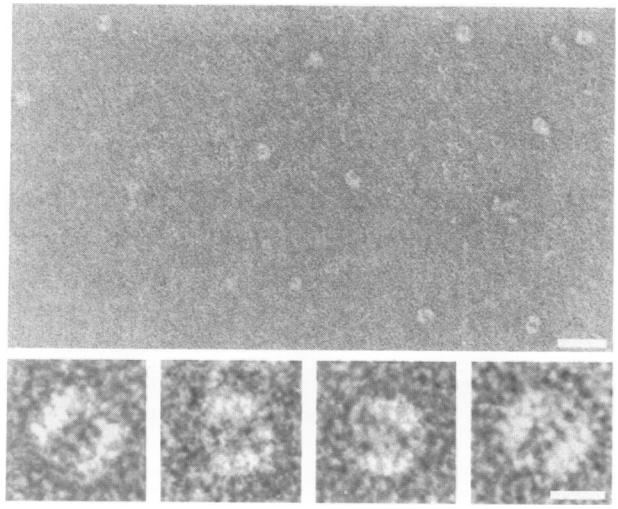

Fig. 5. Structure of axonin-1 as revealed by negative staining electron microscopy. The upper panel shows a field of axonin-1 molecules, and the bottom row shows a gallery of selected axonin-1 molecules at higher magnification. The uniform appearance of the horseshoe-shaped structures suggests little segmental flexibility. Bars = 50 nm for upper panel, 5 nm for bottom row.

et al., 1991). However, a direct interaction between adsorbed axonin-1 and growth cone NgCAM was not shown. At that time, we could not exclude the possibility that, despite the interaction of axonin-1- and NgCAM-coated Covaspheres, adsorbed axonin-1 exerts its neurite outgrowth-promoting activity via an interaction with a growth cone receptor other than NgCAM and that anti-NgCAM Fab perturb this activity more indirectly. The results presented here suggest that the NgCAM binding site of membrane-bound axonin-1 is not accessible for NgCAM of an apposed membrane and prompt a reconsideration of the assumption that axonin-1 substratum exerts its neurite outgrowth-promoting effect by a direct binding to NgCAM of the growth cone. To address this point, we analysed the neurite outgrowth activity of native axonin-1 coated onto tissue culture plastic and presented as substratum for dissociated dorsal root ganglion neurons from 10-day-old chicken embryos in the presence of monovalent X9H8 antibody. As already shown, X9H8 was found to block the axonin-1–NgCAM interaction most potently. Although X9H8 Fab bound to adsorbed axonin-1 (data not shown), no perturbation of neurite outgrowth was detected (Figure 8C and E). Moreover, no perturbation of neurite outgrowth was obtained for X7F6 Fab which is also expected to inhibit binding of neuronal NgCAM to adsorbed axonin-1 (Figure 6A; data not shown). In contrast, monovalent polyclonal antibodies directed to axonin-1 completely blocked neurite outgrowth on axonin-1 (Figure 8E) and, as a control, did not inhibit neurite outgrowth on laminin (data not shown). These results suggested that blocking the NgCAM binding site of adsorbed axonin-1 does not interfere with its neurite outgrowth-promoting activity.

In order to confirm this finding, neurite outgrowth was examined on three different axonin-1 variants produced in a myeloma-based expression system (Traunecker *et al.*, 1991a). Previously, we had demonstrated that recombinant axonin-1 generated by this system is highly similar to native axonin-1 with respect to both its structural and

Table I. Epitope mapping of anti-axonin-1 mAbs to the four amino-terminal Ig domains

	V3B3	X7F6	X7H5	X3G12	X7G9	V9H6	X9C12	X9H8
Wild-type	++	++	++	++	++	++	++	++
ΔIg1234	–	–	–	–	–	–	–	–
Ig1234	++	++	++	++	+	++	++	++
ΔIg12	–	–	–	+	++	–	–	–
ΔIg2	++	++	+	++	++	–	–	–
ΔIg23	++	++	+	++	++	–	–	–
ΔIg3	++	++	++	++	++	–	–	–
ΔIg3	++	++	–	–	–	–	–	–
ΔIg4	++	++	–	–	–	–	–	–
Epitope	Ig1	Ig1	Ig1/4	Ig4	Ig4	Ig1–4	Ig1–4	Ig1–4

Binding of mAbs to wild-type axonin-1 and axonin-1 domain deletion mutants expressed on the surface of COS cells was vizualized by immunofluorescence analysis using FITC-conjugated anti-mouse IgG antibody. Strong immunofluorescence is indicated by '++', weak immunofluorescence by '+' and no immunofluorescence by '–'. In the last row the deduced epitope location is given.

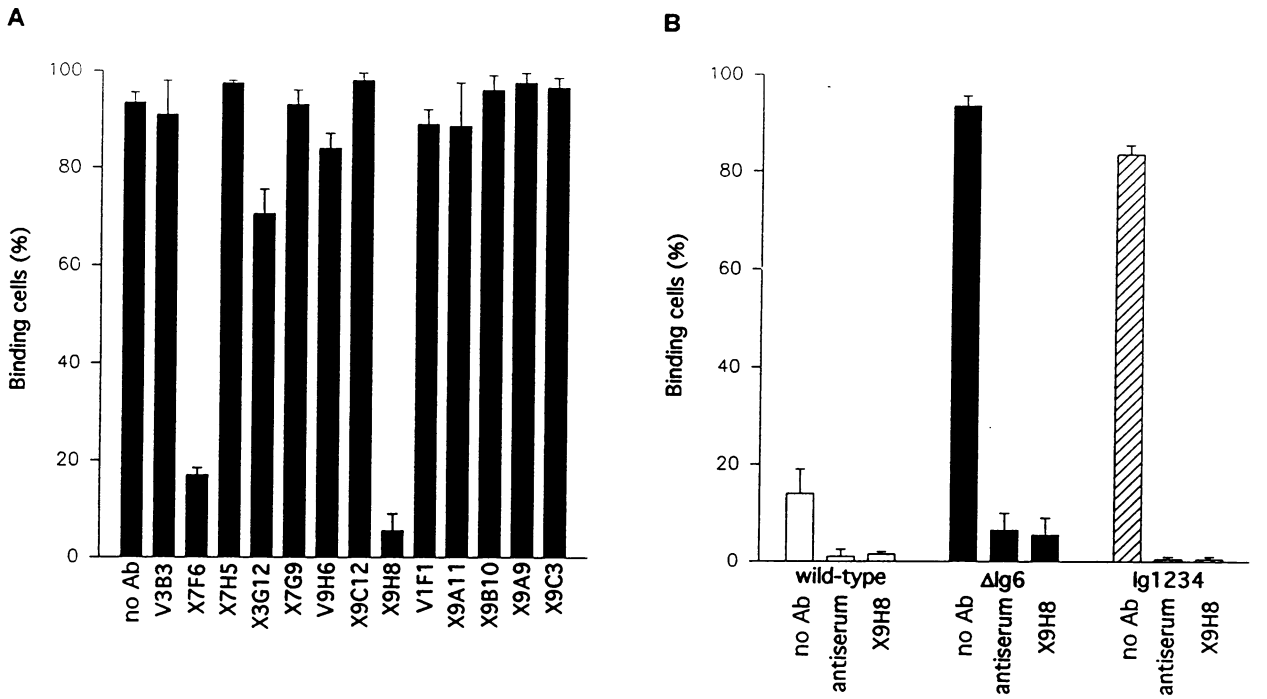

Fig. 6. Interference of anti-axonin-1 mAbs with NgCAM binding. (**A**) Interference of 13 selected anti-axonin-1 mAbs with the binding of NgCAM-conjugated Covaspheres by axonin-1 mutant ΔIg6 transiently expressed on the surface of COS cells. Cells expressing ΔIg6 were pre-incubated with IgG of mouse anti-axonin-1 mAbs that did not bind NgCAM. After binding of NgCAM-conjugated TRITC Covaspheres and fixation, ΔIg6-expressing cells that had bound the antibody were visualized by a FITC-conjugated anti-mouse IgG antibody. The first column ('no Ab') indicates the NgCAM binding of untreated ΔIg6. The first eight mAbs, namely V3B3, X7F6, X7H5, X3G12, X7G9, V9H6, X9C12 and X9H8, bind to epitopes located in the four amino-terminal Ig domains of axonin-1 (Table I). The epitopes of V1F1, X9A11, X9B10, X9A9 and X9C3 were mapped to the axonin-1 domains Ig5, Fn1, Fn2, Fn3 and Fn4, respectively. Quantitative analysis was carried out as described for Figure 2. Columns represent the mean of two independent experiments (error bars indicate SD). *t*-test analysis revealed that results obtained with mAbs V3B3, X7H5, X7G9, V9H6, X9C12, V1F1, X9A11, X9B10, X9A9 and X9C3 do not show a significant difference from the control ($P>0.05$), while results derived from mAbs X7F6 ($P<0.001$), X3G12 ($P<0.05$) and X9H8 ($P<0.002$) are statistically different from the control. (**B**) In addition to axonin-1 mutant ΔIg6, the anti-axonin-1 mAb X9H8 also blocked NgCAM binding by wild-type axonin-1 and axonin-1 mutant Ig1234, and is as potent as polyclonal antibodies to axonin-1. The interference of mAb X9H8 with NgCAM binding of wild-type axonin-1 (open columns), ΔIg6 (solid columns) and Ig1234 (hatched columns) is shown in comparison with goat polyclonal IgG raised against axonin-1 ('antiserum').

functional integrity (Rader *et al.*, 1993). To obtain soluble axonin-1 variants, the four amino-terminal Ig domains, a variant lacking the four amino-terminal Ig domains and wild-type axonin-1 were fused to the Ig C_κ domain of the mouse Ig light chain to generate Ig1234–C_κ, ΔIg1234–C_κ and wild-type–C_κ, respectively (Figure 8A). The soluble axonin-1 variants were constitutively secreted by transfected J558L myeloma cells, immunoaffinity purified with an anti-C_κ mAb, and analysed by SDS–PAGE (Figure 8B). The purified axonin-1 variants were conjugated to fluorescent Covaspheres and analysed for their NgCAM binding capability. As expected, only Covaspheres conjugated with wild-type–C_κ or Ig1234–C_κ but not ΔIg1234–C_κ formed mixed aggregates with NgCAM-conjugated Covaspheres (data not shown). This result further confirmed the mapping of the NgCAM binding site to the four amino-terminal Ig domains of axonin-1 and, in addition, revealed the structural and functional integrity of the soluble axonin-1–C_κ fusion products. To test for neurite outgrowth-promoting activity, the soluble

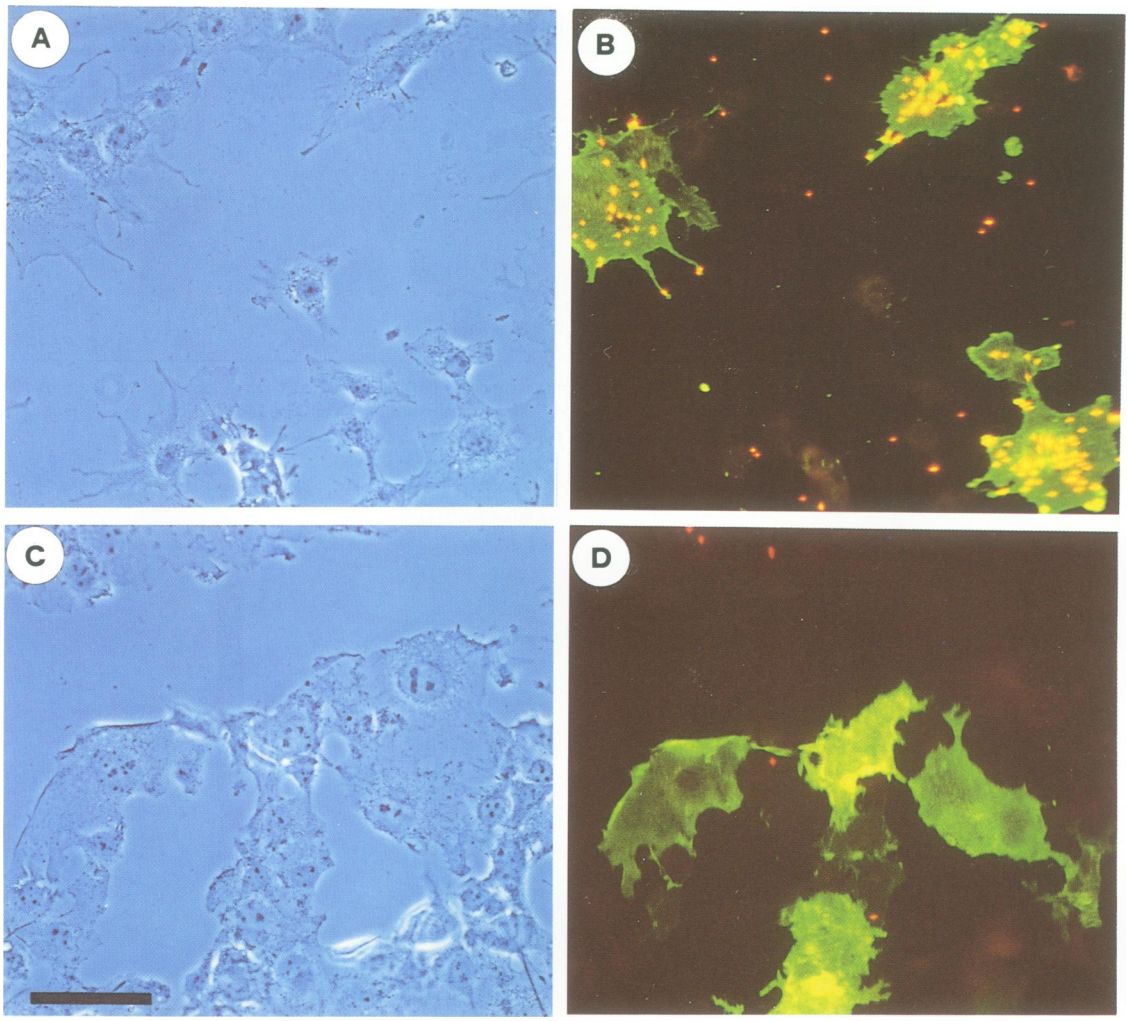

Fig. 7. Interference of anti-axonin-1 mAb X9H8 with the binding of NgCAM-conjugated Covaspheres by axonin-1 mutant Ig1234 expressed on the surface of transiently transfected COS cells. (**A**) and (**B**) COS cells expressing the axonin-1 mutant Ig1234 were detected microscopically after binding of NgCAM-conjugated TRITC Covaspheres and fixation by indirect immunofluorescence using polyclonal antibodies to axonin-1 and a secondary FITC-conjugated antibody. (**C**) and (**D**) Ig1234-expressing COS cells were pre-incubated with IgG of the mouse anti-axonin-1 mAb X9H8. After binding of NgCAM-conjugated TRITC Covaspheres and fixation, Ig1234-expressing cells that had bound the antibody were detected by a FITC-conjugated anti-mouse IgG antibody. (A) and (C) Phase contrast optics. (B) and (D) Optics for simultaneous detection of FITC and TRITC fluorescence. Bar = 100 μm.

axonin-1 variants were coated onto tissue culture plastic and presented as substratum for dissociated dorsal root ganglion neurons from 10-day-old chicken embryos. While the number of neurons with neurites on wild-type–C_κ and ΔIg1234–C_κ was comparable with native axonin-1, Ig1234–C_κ was found to have strongly reduced outgrowth-promoting activity in the range of ovalbumin substratum (Figure 8E). Compared with native axonin-1, purified by the four-step chromatographic procedure established by Ruegg *et al.* (1989), the neurite length on both wild-type–C_κ and ΔIg1234–C_κ was slightly lower (data not shown). We also have observed a reduction of neurite length for immunoaffinity-purified native and recombinant axonin-1 and ascribe it to the relatively harsh conditions which have to be used for eluting proteins from immunoaffinity columns (Rader *et al.*, 1993; data not shown). As for native axonin-1, neurite outgrowth on wild-type–C_κ and ΔIg1234–C_κ could be inhibited specifically by the presence of monovalent polyclonal antibodies directed to axonin-1, whereas addition of X9H8 Fab had no effect (Figure 8E). Taken together, these data show that the four amino-terminal Ig domains of axonin-1 which include the NgCAM binding site are not necessary for neurite outgrowth on axonin-1 substratum.

Discussion

A domain conglomerate of the four amino-terminal Ig domains forms the NgCAM binding site of axonin-1

The localization of the NgCAM binding site of axonin-1 was investigated by a combination of domain deletion mutants and mAbs. This strategy was in part guided by structure/function analyses of ICAM-1, a cell adhesion molecule of the Ig superfamily expressed in the immune system, in which domain deletion studies had revealed that individual domains exhibit distinct ligand binding properties (Staunton *et al.*, 1990; Diamond *et al.*, 1991). To ensure that domains adjacent to the deletion remained intact with regard to their primary structure, we have

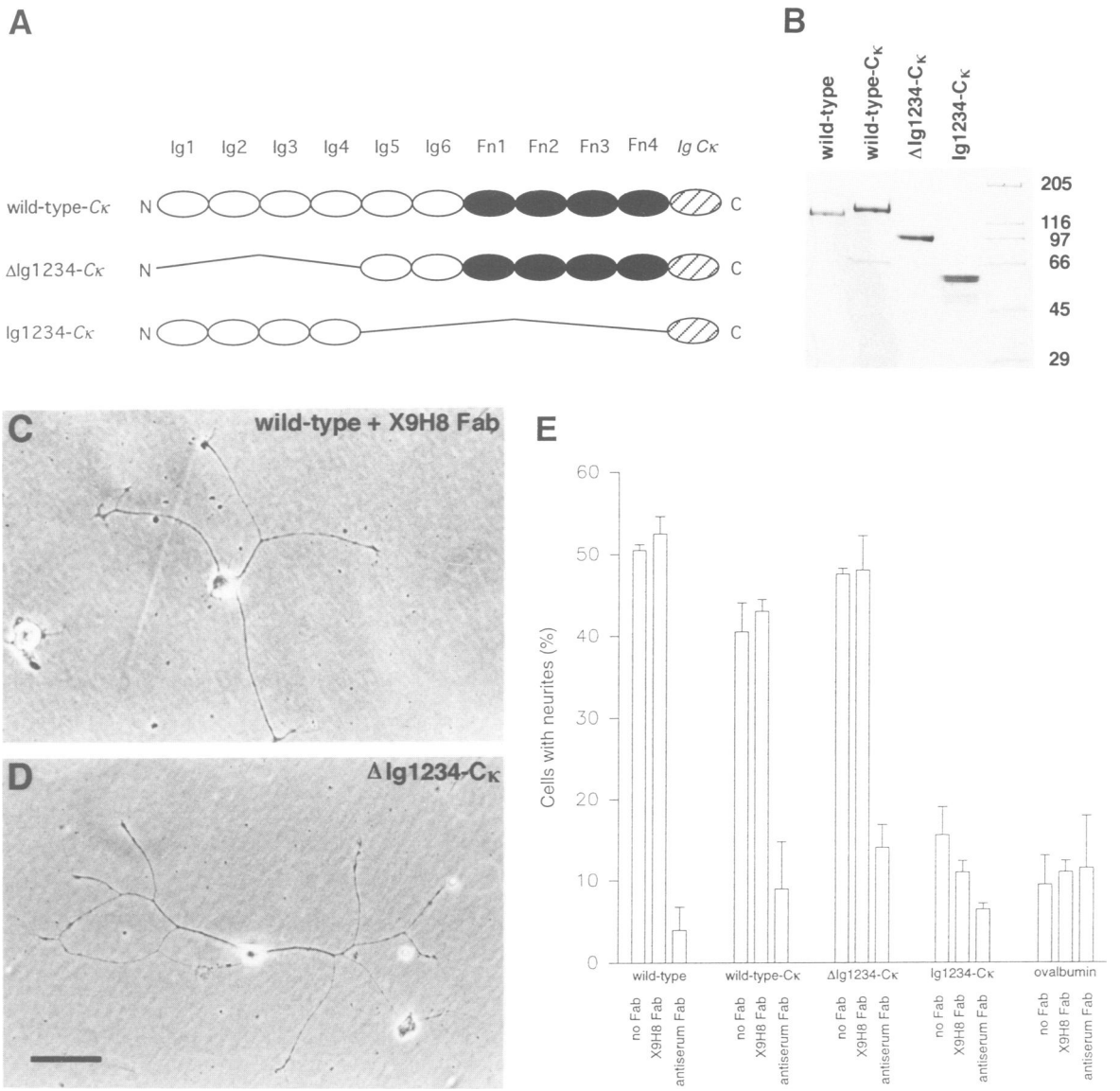

Fig. 8. Localization of the neurite outgrowth-promoting segment of axonin-1 in relation to the NgCAM binding site. (**A**) Schematic representation of soluble axonin-1 variants fused to the Ig C_κ domain (hatched ellipse). For symbols and labels see Figure 2. (**B**) The molecules were stably expressed by myeloma cells, purified from supernatants by affinity chromatography using an anti-C_κ mAb, and analysed on SDS–PAGE (7.5%) after staining with Coomassie Blue. Numbers on the right indicate the molecular masses of marker proteins in kDa. The faint staining of an additional protein band at 66 kDa in the wild-type–C_κ preparation presumably represents traces of serum albumin. The faint staining of additional protein bands at ~50 kDa in the Ig1234–C_κ preparation represents traces of decomposition products of Ig1234–C_κ, as demonstrated by immunoblotting (data not shown). (**C**) Neurite outgrowth of dissociated chicken embryonic dorsal root ganglion neurons on native axonin-1 substratum in the presence of monovalent anti-axonin-1 mAb X9H8. After 22 h in culture, the cells were fixed and photographed using phase contrast optics. (**D**) Neurite outgrowth on ΔIg1234–C_κ substratum. Bar = 50 µm. (**E**) Quantification of neurite outgrowth. The percentage of cells with neurites longer than two cell body diameters was determined on native axonin-1 ('wild-type'), wild-type–C_κ, ΔIg1234–C_κ, Ig1234–C_κ and, as negative control, ovalbumin. Fab of anti-axonin-1 mAb X9H8 or Fab of axonin-1 antiserum were added to a final concentration of 30 or 300 µg/ml, respectively. Columns represent the mean of two independent experiments (error bars indicate SD).

excised the domains precisely at their borders by oligonucleotide-directed mutagenesis. When the domain deletion mutants were used for the mapping of ~100 mAbs directed to axonin-1, an unequivocal assignment was possible for the fifth and sixth Ig domain and the four FNIII domains. With deletions of the four amino-terminal Ig domains, however, approximately one half of the mAbs did not bind if any of the four domains was absent, whereas the others were localized either to the first or the fourth but never to the second or third Ig domain (Table I; data not shown). As the most straightforward interpretation of these results, we postulate that the first and the fourth Ig domain can assume a native structure independently of the presence of the other domains, whereas the second and the third Ig domain maintain their spatial structure only within the intact conglomerate. Thus, the antibodies that recognize only the intact conglomerate, but not the mutants with deletions of one of the four amino-terminal domains, are likely to be directed to the second or third Ig domains.

The binding analyses of NgCAM-conjugated microspheres to axonin-1 domain deletion mutants expressed at

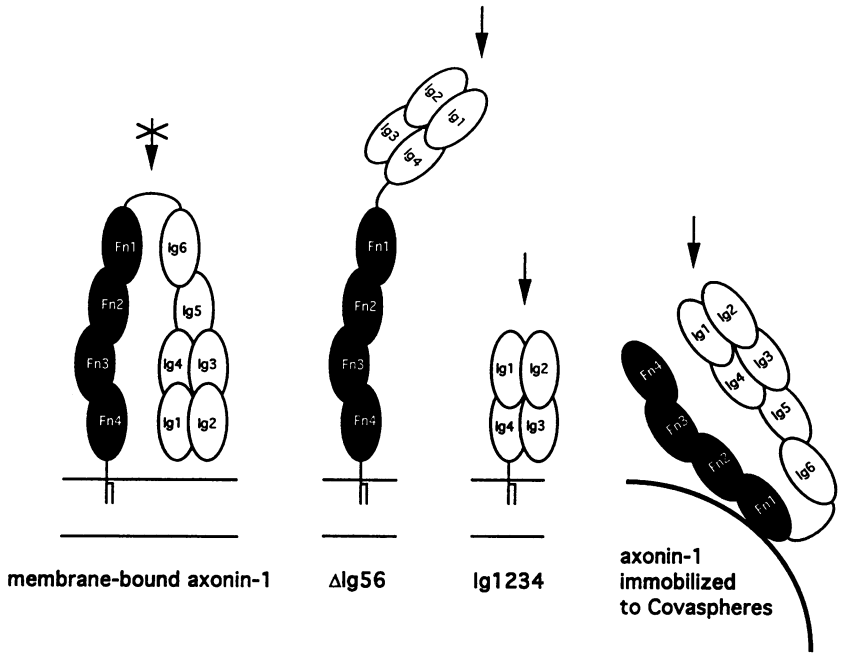

Fig. 9. Model of the domain arrangement of axonin-1. Based on the finding that a deletion of the fifth and sixth amino-terminal Ig domain of axonin-1 results in an increased NgCAM binding, a model for the domain arrangement of axonin-1 is proposed. By means of the glycine/proline-rich segment which separates Ig and FNIII parts, the six Ig domains fold back towards the membrane. The four amino-terminal Ig domains (Ig1, Ig2, Ig3 and Ig4) are shown in close physical association. This conglomerate bears the NgCAM binding site. It is inaccessible to NgCAM presented on either an opposing cell surface or on Covaspheres (arrow). Mutants having Ig5 and/or Ig6 deleted unmask the NgCAM binding site as shown for the axonin-1 mutants ΔIg56 and Ig1234. When axonin-1 is coupled by an amino group-reactive agent to the surface of polystyrene microspheres, the NgCAM binding site is expected to be surface oriented in at least a fraction of the axonin-1 molecules, explaining the pronounced axonin-1–NgCAM interaction found with axonin-1- and NgCAM-conjugated Covaspheres (Kuhn *et al.*, 1991).

the surface of COS cells revealed the NgCAM binding site to reside within the four amino-terminal Ig domains. The entirety of this substructure was required for NgCAM binding. Together with the conclusions drawn from the mAb epitope mapping studies, these results strongly support the idea that these domains form a domain conglomerate. The blocking effects of two mAbs with defined binding locations allowed a further localization of the NgCAM binding site. mAb X9H8, which was found to interfere most strongly with the NgCAM binding of axonin-1, belongs to the group of mAbs that require the entirety of the amino-terminal domain conglomerate for binding and, thus, presumably binds to the second or third Ig domain or to domain borders involving the second or third Ig domain or both. NgCAM binding also is blocked by mAb X7F6 which was mapped to the first Ig domain. Thus, the first and at least one of the two following domains appear to be involved in the structure of the NgCAM binding site. Based on domain deletion mutants and mAb epitope mapping, the NgCAM binding site of F11, a close relative of axonin-1 exhibiting 52.5% amino acid sequence identity, was mapped to the two amino-terminal Ig domains (Brümmendorf *et al.*, 1993). However, the smallest F11 domain deletion mutant with NgCAM binding activity included all four amino-terminal Ig domains. Thus, the entirety of this substructure seems to be necessary for NgCAM binding by both axonin-1 and F11. In consideration of these results, it appears likely that the NgCAM binding sites of axonin-1 and F11 are related if not identical.

A model of the domain arrangement of axonin-1

The domain conglomerate of the four amino-terminal Ig domains was found to be necessary and sufficient for NgCAM binding. Surprisingly, the construct comprising these four Ig domains directly coupled to the GPI anchor exhibited markedly increased binding as compared with wild-type axonin-1, suggesting that parts of the axonin-1 structure beyond the four amino-terminal Ig domains exert a strong inhibitory influence on the NgCAM binding function of the domain conglomerate. Domain deletion studies in the region distal to the conglomerate identified the fifth and the sixth Ig domain as crucial for this inhibitory effect. Strongly increased NgCAM binding was observed with the single domain deletion mutants ΔIg5 and ΔIg6, and with all double domain deletions combining either ΔIg5 or ΔIg6 with single domain deletions beyond the four amino-terminal Ig domains. Clearly, the weak binding of NgCAM-conjugated microspheres to membrane-bound axonin-1 correlates with the presence of the fifth and sixth Ig domain of axonin-1. Based on these results and on electron micrographs which suggest a horseshoe-shaped structure of axonin-1, we present a model of the domain arrangement of axonin-1 (Figure 9). As a main feature of this model, the six Ig domains, including a conglomerate of the four amino-terminal Ig domains, fold back towards the membrane, possibly by means of the highly conserved glycine/proline-rich segment between the Ig and the FNIII moieties (Furley *et al.*, 1990; Zuellig *et al.*, 1992; Hasler *et al.*, 1993). Due to the backfolding, the amino-terminal domain conglomerate

containing the NgCAM binding site becomes located close to the membrane-anchored carboxy-terminal domains and, thus, may be inaccessible for NgCAM exposed on the surface of another cell. Conversely, when axonin-1 is coupled randomly to microspheres, the NgCAM binding site is expected to be surface oriented in at least a fraction of the axonin-1 molecules (Figure 9), explaining the strong binding to NgCAM observed in these experiments (Kuhn *et al.*, 1991; Rader *et al.*, 1993). Bulky and charged sugar residues located on the fifth and sixth domain might contribute to the inaccessibility of the NgCAM binding site of membrane-bound axonin-1, as suggested by the fact that four out of eight potential *N*-glycosylation sites conserved among axonin-1 and its mammalian homologues are concentrated on the fifth and sixth Ig domain (Hasler *et al.*, 1993). In addition to deletions involving the fifth and sixth Ig domain, domain deletion mutant ΔFn4 was found to have increased NgCAM binding compared with wild-type axonin-1. Assuming a stabilization of the backfolded shape by an intramolecular interaction near to the membrane, e.g. by a physical association of the first Ig and the fourth FNIII domain, the increased NgCAM binding by the axonin-1 mutant ΔFn4 could be ascribed to a destabilization of the backfolded shape resulting in an improved accessibility of the NgCAM binding site. A stabilization of the backfolded shape by an intramolecular interaction of axonin-1 is also suggested by the electron micrographs. In contrast to NCAM (Becker *et al.*, 1989) and ICAM-1 (Staunton *et al.*, 1990), electron micrographs of axonin-1 revealed only little segmental flexibility.

The electron micrographs of axonin-1 at the presently available resolution support the backfolded shape but do not allow a more detailed description of the tertiary structure of axonin-1. In particular, it is important to note that the structural features of the detailed domain arrangement of axonin-1 as depicted in Figure 9 are based on the NgCAM binding site mapping by axonin-1 domain deletion mutants and on the epitope mapping of anti-axonin-1 mAbs.

A reconsideration of the molecular interaction involved in neurite outgrowth on axonin-1 substratum

A major conclusion drawn from the membrane-proximal location of the NgCAM binding site of axonin-1 might be that axonin-1 and NgCAM interact in the plane of the same membrane (*in cis*) rather than across the intermembrane space (*in trans*). This prediction is supported by several independent observations. (i) When TAG-1 and L1, the putative rodent homologues of axonin-1 and NgCAM, were expressed on the surface of *Drosophila* Schneider 2 cells, no interaction *in trans* occurred, as indicated by the observation that the cells did not form mixed aggregates (Felsenfeld *et al.*, 1994). (ii) Evidence for an interaction of axonin-1 and NgCAM *in cis* is derived from observations of co-clustering (Stoeckli *et al*, 1993) and cross-linking (S.Kunz and P.Sonderegger, in preparation) of axonin-1 and NgCAM in the plane of the same membrane. (iii) Neurite outgrowth studies in the presence of anti-axonin-1 mAbs that interfere with NgCAM binding and on truncated forms of axonin-1 show that the neurite outgrowth-promoting activity of axonin-1 substratum is not mediated by an axonin-1–NgCAM interaction *in trans*.

As determined by the neurite outgrowth studies on truncated forms of axonin-1, the growth cone receptor for axonin-1 substratum binds axonin-1 in a region distal to the four amino-terminal Ig domains that form the NgCAM binding site. Candidates for this axonin-1 receptor include the currently identified axonin-1 ligands, namely axonin-1 itself (Rader *et al.*, 1993) and NrCAM/Bravo (Suter *et al.*, 1995). In addition, an $\alpha\beta_1$ integrin was reported to be involved in neurite outgrowth on TAG-1 substratum (Felsenfeld *et al.*, 1994). The fact that polyclonal antibodies directed to L1/NgCAM interfere with neurite outgrowth on TAG-1/axonin-1 substratum (Kuhn *et al.*, 1991; Felsenfeld *et al.*, 1994) suggests that neuronal L1/NgCAM is involved in neurite outgrowth on TAG-1/axonin-1 substratum. On the one hand, we cannot exclude the possibility that polyclonal antibodies binding to L1/NgCAM trigger an intracellular signal that reverses the signal induced by TAG-1/axonin-1 substratum; indeed, it is known that polyclonal and at least one monoclonal antibody directed to L1 are capable of triggering intracellular signals (Appel *et al.*, 1995). On the other hand, it is conceivable that neuronal L1/NgCAM is directly involved in neurite outgrowth on TAG-1/axonin-1 substratum by an interaction *in cis* with the neuronal receptor of adsorbed TAG-1/axonin-1. Networks of molecules interconnected in the plane of the membrane and across the intermembrane space have been proposed as powerful means of regulating the growth and the guidance of axons during neurogenesis (Sonderegger and Rathjen, 1992). The elucidation of the domain arrangement and the mapping of the binding sites of the participating molecules provides a basis for future investigations of the molecular composition and structure of these networks.

Materials and methods

Materials

Native axonin-1 was purified from the vitreous fluid of 14-day-old chicken embryos (Ruegg *et al.*, 1989). NgCAM was isolated from 14-day-old chicken brain membranes by immunoaffinity chromatography using an anti-NgCAM mAb provided by Dr F.G.Rathjen (Rathjen *et al.*, 1987). Goat and rabbit polyclonal and mouse monoclonal antibodies against axonin-1 were raised as previously described (Ruegg *et al.*, 1989). IgG and Fab were obtained as previously specified (Stoeckli *et al.*, 1991).

Construction of axonin-1 deletion mutants

A 2.2 kb *Sac*I–*Hin*dIII fragment, a 1.7 kb *Eco*RI–*Hin*dIII fragment, a 0.6 kb *Bam*HI–*Hin*dIII fragment and a 1.1 kb *Hin*dIII fragment were isolated from the axonin-1 expression vector pMAX which contains the entire coding region of the axonin-1 cDNA (Rader *et al.*, 1993). The fragments were cloned into the phagemid vector pTZ19U (Bio-Rad Laboratories, Richmond, CA) generating pTZ19U/axS-H, pTZ19U/axE-H, pTZ19U/axB-H and pTZ19U/axH-H, respectively. pTZ19U/axB-H-H was generated by cloning the 1.1-kb *Hin*dIII fragment into pTZ19U/axB-H. Uracil-containing single strand DNA as a template for *in vitro* mutagenesis was obtained by using the *Escherichia coli* strain CJ 236 (Bio-Rad) and the helper phage VCSM13 (Stratagene, La Jolla, CA) as described (Yuckenberg *et al.*, 1991). The 10 single domain deletions were made by loop-out oligonucleotide-directed mutagenesis using the following oligonucleotides: CRΔIg1, 5′-TCTGGTGCCAAGCACAGA-GTGGCGGCTTTTTGCAGGAATTCTCTGCAG-3′; CRΔIg2, 5′-GGG-AAGCATCCCTCCGCTTTGGCGACGCCAGGCAGTATGCACCCAG-3′; CRΔIg3, 5′-CCAGCTCAGCCTGGCTGCCGAGGCTCAGCCGG-ACTGGCTGGATG-3′; CRΔIg4, 5′-TACCAGGGCCGCATCATCATT-CACGCCTTAGCACCAGATTTTAGACTAAAC-3′; CRΔIg5, 5′-CAA-

GTGCTGAATTAACAGTGCAAGCCGATGCCACCAAAATCACACT-GGCAC-3′; CRΔIg6, 5′-AGCACGGGGATCCTCTCTGTTCGAG-CCACGCTGACTGTCAGAGGACC-3′; RLΔFn1, 5′-GCCACGCT-GACTGTCAGAGGACCCACGGTGGCACCATCTGGGCTCGGC-3′; RLΔFn2, 5′-CGTACCAAAGAAGCAGCACCCAAGGTGGCACCA-TTCAGAGTTACGGCCAAAGCC-3′; RLΔFn3, 5′-GTGTACTCT-GCAGAAGAAGAACCAAGGAGGCCACCAGGCAACATCTCC-3′; RLΔFn4, 5′-AACATCACGACCACAAAGCCACCAACCAGTATGA-TGGTGGAAGACTCC-3′.

Oligonucleotide phosphorylation, annealing and second-strand synthesis were performed as described (Yuckenberg *et al.*, 1991) using pTZ19U/axS-H as a template for CRΔIg1 and CRΔIg2, pTZ19U/axE-H for CRΔIg3, CRΔIg4, CRΔIg5 and CRΔIg6, pTZ19U/axB-H-H for RLΔFn1, and pTZ19U/axH-H for RLΔFn2, RLΔFn3 and RLΔFn4. All other deletions were made by introducing *Eco*RI sites at different locations. CRE1 (5′-AGCTACGGGCCGGAATTCGAGGAGCAGCC-AGC-3′) introduced an *Eco*RI site in front of the Ig1 coding region, CRE2 (5′-CTGGCTGCCGAGGAATTCAGGCAGTATGCACC-3′) at the Ig2/Ig3 border, CRE3 (5′-CACGCTCAGCCGGAATTCCTGGATGTGAT-CACG-3′) at the Ig3/Ig4 border, CRE4 (5′-GCTGAATTAACAGTGC-AAGAATTCGCACCAGATTTTAGAC-3′) at the Ig4/Ig5 border and CRE/GPI (5′-GACCCCAGCAGAATTCCACATCGTCCG-3′) between Fn4 and the sequence responsible for GPI anchorage. *In vitro* mutagenesis was performed as described above using pTZ19U/axS-H as a template for CRE1, pTZ19U/axE-H for CRE2, CRE3 and CRE4, and pTZ19U/axH-H for CRE/GPI. By use of the generated *Eco*RI sites in addition to the natural *Eco*RI site at the Ig1/Ig2 border, the deletion mutants ΔIg12, ΔIg23, ΔIg34, ΔIg1234 and Ig1234 were generated by depletion of the respective *Eco*RI fragments. Due to the *Eco*RI insertions, the latter constructs led to conservative amino acid substitutions (see below). All deletion mutants were verified by double-strand DNA sequencing and cloned into the expression vector pSCT-axonin-1 which drives the axonin-1 expression under the cytomegalovirus promoter and contains an SV40 origin of replication. To generate the double deletions ΔIg51, ΔIg52, ΔIg53, ΔIg5Fn1, ΔIg5Fn2, ΔIg5Fn3, ΔIg5Fn4, ΔIg61, ΔIg62, ΔIg63, ΔIg64, ΔIg6Fn2, ΔIg6Fn3 and ΔIg6Fn4, single deletions were combined by substituting appropriate restriction fragments. Neighboured double domain deletions were generated as follows and verified by double-strand DNA sequencing: ΔIg54 by ligation of *Bcl*I at the beginning of the Ig4 coding region to *Bam*HI at the end of Ig5 using pSCT-axonin-1 produced in the dam⁻ *E.coli* strain GM33; ΔIg56 by ligation of *Eco*RV at the beginning of Ig6 to *Sma*I at the beginning of Fn1 using pSCT-axonin-1/ΔIg5; and ΔIg6Fn1 by ligation of *Sma*I at the beginning of Fn1 to Klenow-treated *Hin*dIII at the end of Fn1 using pSCT-axonin-1/ΔIg6.

Summary of the obtained mutants by their amino acid variation compared with wild-type axonin-1 (Zuellig *et al.*, 1992): ΔIg1 = Δ(M27–F124); ΔIg2 = Δ(F126–E227); ΔIg3 = Δ(D228–H319); ΔIg4 = Δ(A320–Q408); ΔIg5 = Δ(L410–R501); ΔIg6 = Δ(D502–S594); ΔFn1 = Δ(P603–P705); ΔFn2 = Δ(T706–P807); ΔFn3 = Δ(K808–P908); ΔFn4 = Δ(P907–G1001); ΔIg12 = Δ(M27–F124; S131–A229); ΔIg23 = Δ(S131–W324); ΔIg34 = Δ(A229–A409), D228E, L410F; ΔIg1234 = Δ(M27–F124; S131–L410); Ig1234 = Δ(A409–A992), V994F; ΔIg51 = Δ(M27–F124; L410–R501); ΔIg52 = Δ(F126–E227; L410–R501); ΔIg53 = Δ(D228–H319; L410–R501); ΔIg54 = Δ(T329–G496); ΔIg56 = Δ(L410–R501; I515–P603); ΔIg5Fn1 = Δ(L410–R501; P603–P705); ΔIg5Fn2 = Δ(L410–R501; T706–P807); ΔIg5Fn3 = Δ(L410–R501; K808–P908); ΔIg5Fn4 = Δ(L410–R501; P907–G1001); ΔIg61 = Δ(M27–F124; D502–S594); ΔIg62 = Δ(F126–E227; D502–S594); ΔIg63 = Δ(D228–H319; D502–S594); ΔIg64 = Δ(A320–Q408; D502–S594); ΔIg6Fn1 = Δ(D502–S594; G604–P691); ΔIg6Fn2 = Δ(D502–S594; T706–P807); ΔIg6Fn3 = Δ(D502–S594; K808–P908); ΔIg6Fn4 = Δ(D502–S594; P907–G1001).

Transfection of COS-1 cells

Transient transfectants were obtained by electroporation according to Chu *et al.* (1987) and Rols *et al.* (1994). In brief, 10^6 trypsinized COS-1 cells were resuspended in 700 μl of phosphate-buffered saline (PBS; 137 mM NaCl, pH 7.4, 3 mM KCl, 8 mM Na_2HPO_4, 1.5 mM KH_2PO_4) and mixed with 100 μl of PBS containing 10 μg of CsCl-purified vector DNA. After a 10 min incubation on ice, electroporation was carried out in a 1 cm cuvette by applying 960 μF and 230 V (Bio-Rad Gene Pulser). Post-incubation was for 10 min at 37°C. Then, the cells were cultured on 28 cm^2 cell culture dishes in 5 ml of Dulbecco's modified Eagle's medium (DMEM) supplemented with 10% fetal calf serum (FCS) at 37°C in 5% CO_2. After 7 h, the cells were washed twice with PBS and incubated overnight with 10 ml of DMEM, 10% FCS.

For immunoblotting the cells were washed twice with PBS and detached by treatment with 2 mM EDTA in PBS 2 days after transfection. For solubilization of membrane proteins, detached cells were sonicated with 10 pulses (20 W, 1 s) using a microtip sonifier (Branson Sonic Power Co., Danbury, CT). The membranes were sedimented by ultracentrifugation at 200 000 *g* for 20 min at 4°C and solubilized with 2% SDS. Immunoblotting was performed using 10 μl of solubilized membranes corresponding to ~10^4 COS cells per lane. For comparison, 5 μl of vitreous fluid of 14-day-old chicken embryos was blotted. Immunodetection was carried out with mixtures of four mouse monoclonal antibodies against axonin-1 and goat anti-mouse IgG conjugated to peroxidase (Kirkegaard & Perry Laboratories, Inc., Gaithersburg, MD) at a dilution of 1:1000.

Binding of NgCAM-coated Covaspheres to transfected COS-1 cells and immunofluorescence staining

One day after transfection, cells were washed twice with PBS, detached by treatment with 2 mM EDTA in PBS, and resuspended in DMEM, 10% FCS. The cells were cultured overnight on polylysine-coated glass Lab-Tek slides (Nunc Inc., Naperville, IL) at 37°C in 5% CO_2. Two days after transfection, the cells were washed twice with DMEM, 5 mg/ml bovine serum albumin (BSA). NgCAM-coated tetramethylrhodamine isothiocyanate (TRITC) Covaspheres (Kuhn *et al.*, 1991) were sonicated for 2 min, diluted 1:1000 in DMEM, 5 mg/ml BSA and again sonicated for 3 min immediately before use. The cells were incubated with the prepared Covaspheres for 1 h at 37°C in 5% CO_2, washed twice with DMEM, 5 mg/ml BSA, and fixed with 2% formaldehyde (Fluka Chemie AG, Buchs, Switzerland) for 1 h at 37°C. After washing twice with PBS, 1% FCS, axonin-1-expressing cells were detected by indirect immunofluorescence staining using goat antiserum raised against axonin-1 (1:1000 dilution) and fluorescein isothiocyanate (FITC)-conjugated rabbit anti-goat IgG (1:100 dilution; Zymed Laboratories Inc., South San Francisco, CA). The preparation was examined with a fluorescence microscope (Leitz DMR; Leica AG, Heerbrugg, Switzerland) using a G/R filter (Leica) for simultaneous detection of FITC and TRITC fluorescence. For quantification, green fluorescing cells binding at least three red fluorescing Covaspheres were scored as binding cells (non-expressing cells were found to bind 0–1 Covaspheres) and 100 cells were scored in all. In antibody blocking experiments, the cells were pre-incubated for 2 h at 37°C with IgG of mouse monoclonal or goat polyclonal antibodies at a concentration of 30 or 500 μg/ml, respectively, in DMEM, 1% FCS. Incubation with NgCAM-coated TRITC Covaspheres and fixation was carried out as described above. Axonin-1-expressing cells that had bound the antibodies were detected by incubation with FITC-conjugated goat anti-mouse IgG (1:200 dilution; Cappel; Organon Teknika nv, Turnhout, Belgium) or FITC-conjugated rabbit anti-goat IgG (1:100 dilution; Zymed), respectively.

Myeloma-based production of soluble axonin-1 variants

For wild-type–C_k, the cDNA fragment CR2F-HB3 was amplified by PCR using the full-length axonin-1 cDNA clone d-509 as a template (Zuellig *et al.*, 1992) and the primer pair CR2F (Rader *et al.*, 1993) and HB3 (5′-GCCAAGCTTACTTACCTCCACTGTTTCGGACGATG-3′). PCR amplification was performed as previously described (Rader *et al.*, 1993). CR2F-HB3 was digested with *Hin*dIII and used to substitute the *Hin*dIII fragment of the axonin-1 coding region in pMAX (Rader *et al.*, 1993). This substitution fused the axonin-1 coding region to the exon encoding the Ig-κ constant region (Ig C_K). For a vector map of pMAX which is derived from pCD4-FvCD3-C_K (Traunecker *et al.*, 1991b) see Rader *et al.* (1993).

For Δ1g1234–C_K, the axonin-1 deletion mutant ΔIg1234 was cloned into pMAX generating pMAX/ΔIg1234. *Hin*dIII-digested CR2F-HB3 was cloned into pMAX/ΔIg1234 as described for wild-type–C_K.

For Ig1234–C_k, a *Sac*I site was introduced at the Ig4/Ig5 border by oligonucleotide-directed mutagenesis using pTZ19U/axS-H (see above) as a template for the oligonucleotide CRS4 (5′-GCTGAATTAACA-GTGGGAGCTCTAGCACCAGATTTTAG-3′). A Q408G amino acid substitution resulted from the *Sac*I insertion. The *Sac*I fragment that encodes the start codon, the signal peptide and the four amino-terminal Ig domains of axonin-1 was cloned into *Sac*I-digested pMAX, thereby substituting the entire axonin-1 coding region and fusing the four amino-terminal Ig domains to Ig C_K.

The integrity of the three constructs was confirmed by double-strand DNA sequencing. Stable transfectants were obtained by transfecting the constructs into the mouse myeloma cell line J558L by protoplast fusion (Oi *et al.*, 1983). Selection and screening of transfected myeloma cells was done as previously described (Rader *et al.*, 1993). For isolation of

the axonin-1 variants, transfected myeloma cells were adapted to 1% FCS in DMEM and cultivated in roller bottles (Costar, Cambridge, MA). Supernatants were concentrated by ultrafiltration (Skanette; Skan AG, Basel, Switzerland) and passed through an immunoaffinity column with immobilized rat anti-mouse C_κ mAb 187.1 (American Type Culture Collection, Rockville, MD). Bound antigen was washed with 50 column volumes of PBS and eluted with 50 mM diethylamine. The eluate was neutralized immediately by the addition of 1/5 volume 1 M Tris–HCl, pH 7.0, and dialysed against PBS.

Neurite outgrowth assay

Native axonin-1 and axonin-1 variants at a concentration of 75 μg/ml were adsorbed directly to tissue culture plastic (Nunclon; Nunc) for 2 h at 37°C. After washing with PBS, the tissue culture plastic was blocked for 30 min at 37°C with 10 mg/ml ovalbumin and washed again with PBS. Dissociated dorsal root ganglion neurons from 10-day-old chicken embryos were plated at a density of 70 000 cells/10 cm^2 and cultivated for 22 h in serum-free medium as specified previously (Stoeckli *et al.*, 1991). For antibody perturbation tests, Fab of monoclonal mouse anti-axonin-1 IgG and Fab of polyclonal goat anti-axonin-1 IgG were added to a final concentration of 30 and 300 μg/ml, respectively. After 22 h in culture, the cells were fixed by addition of glutaraldehyde to a final concentration of 2%. Quantification of neurite outgrowth was performed as described by Venstrom and Reichardt (1995). Cells with neurites longer than two cell body diameters were scored as cells with neurites and 100 cells were scored for each condition.

Electron microscopy

Axonin-1 molecules were adsorbed on glow-discharged C-coated EM grids by placing the grids with the C-film facing down on 5 μl drops of a 75 μg/ml dilution of native axonin-1 in 20 mM NaP_i, pH 7.3. After 60 s, the excess liquid was removed and the immobilized molecules stained for 30 s with two sequentially applied drops of 2% uranyl acetate. Finally, excess stain was blotted off with filter paper. After air drying, the grids were examined in a Philips CM12 transmission electron microscope operating at 100 kV acceleration voltage. Micrographs were taken with a Gatan G94 Slow Scan CCD camera under low dose conditions at a magnification of 60 000 and at ~500 nm underfocus. The images were stored on an Apple Macintosh Quadra 950 computer and hard copies were made with a Tektronics II_{SD} sublimation printer.

Acknowledgements

We thank Dr A.J.Furley (London) for valuable comments on the manuscript, Dr R.Jaenicke (Regensburg) for sedimentation-equilibrium ultracentrifugation of axonin-1, D.M.Suter and R.Wepf for initiating the analysis of axonin-1 by electron microscopy, and R.Savoca for axonin-1 purification. This work was supported by grants from the Swiss National Science Foundation, the Bonizzi-Theler-Stiftung, the Sassella Stiftung and the Union Bank of Switzerland on behalf of a client.

References

Amzel,L.M. and Poljak,R.J. (1979) Three-dimensional structure of immunoglobulins. *Annu. Rev. Biochem.*, **48**, 961–997.

Appel,F., Holm,J., Conscience,J.F., von Bohlen und Halbach,F., Faissner,A., James,P. and Schachner,M. (1995) Identification of the border between fibronectin type III homologous repeats 2 and 3 of the neural cell adhesion molecule L1 as a neurite outgrowth promoting and signal transduction domain. *J. Neurobiol.*, **28**, 297–312.

Becker,J.W., Erickson,H.P., Hoffman,S., Cunningham,B.A. and Edelman, G.M. (1989) Topology of cell adhesion molecules. *Proc. Natl Acad. Sci. USA*, **74**, 3345–3349.

Brümmendorf,T. and Rathjen,F.G. (1993) Axonal glycoproteins with immunoglobulin- and fibronectin type III-related domains in vertebrates: structural features, binding activities, and signal transduction. *J. Neurochem.*, **61**, 1207–1219.

Brümmendorf,T., Wolff,J.M., Frank,R. and Rathjen,F.G. (1989) Neural cell recognition molecule F11: homology with fibronectin type III and immunoglobulin type C domains. *Neuron*, **2**, 1351–1361.

Brümmendorf,T., Hubert,M., Treubert,U., Leuschner,R., Tárnok,A. and Rathjen,F.G. (1993) The axonal recognition molecule F11 is a multifunctional protein: specific domains mediate interactions with NgCAM and restrictin. *Neuron*, **10**, 711–727.

Burgoon,M.P., Grumet,M., Mauro,V., Edelman,G.M. and Cunningham, B.A. (1991) Structure of the chicken neuron–glia cell adhesion molecule, Ng-CAM: origin of the polypeptides and relation to the Ig superfamily. *J. Cell Biol.*, **112**, 1017–1029.

Chu,G., Hayakawa,H. and Berg,P. (1987) Electroporation for the efficient transfection of mammalian cells with DNA. *Nucleic Acids Res.*, **15**, 1311–1326.

Connelly,M.A., Grady,R.C., Mushinski,J.F. and Marcu,K.B. (1994) PANG, a gene encoding a neuronal glycoprotein, is ectopically activated by intracisternal A-type particle long terminal repeats in murine plasmacytomas. *Proc. Natl Acad. Sci. USA*, **91**, 1337–1341.

Diamond,M.S., Staunton,D.E., Marlin,S.D. and Springer,T.A. (1991) Binding of the integrin Mac-1 (CD11b/CD18) to the third immunoglobulin-like domain of ICAM-1 (CD54) and its regulation by glycosylation. *Cell*, **65**, 961–971.

Felsenfeld,D.P., Hynes,M.A., Skoler,K.M., Furley,A.J. and Jessell,T.M. (1994) TAG-1 can mediate homophilic binding, but neurite outgrowth on TAG-1 requires an L1-like molecule and β1 integrins. *Neuron*, **12**, 675–690.

Furley,A.J., Morton,S.B., Manalo,D., Karagogeos,D., Dodd,J. and Jessell,T.M. (1990) The axonal glycoprotein TAG-1 is an immunoglobulin superfamily member with neurite outgrowth-promoting activity. *Cell*, **61**, 157–170.

Gennarini,G., Cibelli,G., Rougon,G., Mattei,M.G. and Goridis,C. (1989) The mouse neuronal cell surface protein F3: a phosphatidylinositol-anchored member of the immunoglobulin superfamily related to chicken contactin. *J. Cell Biol.*, **109**, 775–788.

Giger,R.J., Vogt,L., Zuellig,R.A., Rader,C., Henehan-Beatty,A., Wolfer, D.P. and Sonderegger,P. (1995) The gene of chicken axonin-1, complete structure and analysis of the promoter. *Eur. J. Biochem.*, **227**, 617–628.

Goodman,C.S. and Shatz,C.J. (1993) Developmental mechanisms that generate precise patterns of neuronal connectivity. *Cell*, **72**/*Neuron*, **10** (suppl.), 77–98.

Grumet,M., Mauro,V., Burgoon,M.P., Edelman,G.M. and Cunningham, B.A. (1991) Structure of a new nervous system glycoprotein, Nr-CAM, and its relationship to subgroups of neural cell adhesion molecules. *J. Cell Biol.*, **113**, 1399–1412.

Hasler,T.H., Rader,C., Stoeckli,E.T., Zuellig,R.A. and Sonderegger,P. (1993) cDNA cloning, structural features, and eucaryotic expression of human TAG-1/axonin-1. *Eur. J. Biochem.*, **211**, 329–339.

Kayyem,J.F., Roman,J.M., de la Rosa,E.J., Schwarz,U. and Dreyer,W.J. (1992) Bravo/NrCAM is closely related to the cell adhesion molecules L1 and NgCAM and has a similar heterodimer structure. *J. Cell Biol.*, **118**, 1259–1270.

Kuhn,T.B., Stoeckli,E.T., Condrau,M.A., Rathjen,F.G. and Sonderegger,P. (1991) Neurite outgrowth on immobilized axonin-1 is mediated by a heterophilic interaction with L1(G4) *J. Cell Biol.*, **115**, 1113–1126.

Leahy,D.J., Hendrickson,W.A., Aukhil,I. and Erickson,H.P. (1992) Structure of a fibronectin type III domain from tenascin phased by MAD analysis of the selenomethionyl protein. *Science*, **258**, 987–991.

Oi,V.T., Morrison,S.L., Herzenberg,L.A. and Berg,P. (1983) Immunoglobulin gene expression in transformed lymphoid cells. *Proc. Natl Acad. Sci. USA*, **80**, 825–829.

Patterson,P.H. (1992) Process outgrowth and the specificity of connections. In Hall,Z.W. (ed.), *An Introduction to Molecular Neurobiology*. Sinauer Associates, Sunderland, MA, pp. 388–427.

Rader,C., Stoeckli,E.T., Ziegler,U., Osterwalder,T., Kunz,B. and Sonderegger,P. (1993) Cell–cell adhesion by homophilic interaction of the neuronal recognition molecule axonin-1. *Eur. J. Biochem.*, **215**, 133–141.

Ranscht,B. (1988) Sequence of contactin, a 130-kD glycoprotein concentrated in areas of interneuronal contact, defines a new member of the immunoglobulin supergene family in the nervous system. *J. Cell Biol.*, **107**, 1561–1573.

Rathjen,F.G. and Jessell,T.M. (1991) Glycoproteins that regulate the growth and guidance of vertebrate axons: domains and dynamics of the immunoglobulin/fibronectin type III subfamily. *Semin. Neurosci.*, **3**, 297–307.

Rathjen,F.G., Wolff,J.M., Frank,R., Bonhoeffer,F. and Rutishauser,U. (1987) Membrane glycoproteins involved in neurite fasciculation. *J. Cell Biol.*, **104**, 343–353.

Rols,M.-P., Delteil,C., Serin,G. and Teissi,J. (1994) Temperature effects on electrotransfection of mammalian cells. *Nucleic Acids Res.*, **22**, 540.

Ruegg,M.A., Stoeckli,E.T., Kuhn,T.B., Heller,M., Zuellig,R. and Sonderegger,P. (1989) Purification of axonin-1, a protein that is secreted from axons during neurogenesis. *EMBO J.*, **8**, 55–63.

Sonderegger,P. and Rathjen,F.G. (1992) Regulation of axonal growth in

the vertebrate nervous system by interactions between glycoproteins belonging to two subgroups of the immunoglobulin superfamily. *J. Cell Biol.*, **119**, 1387–1394.

Staunton,D.E., Dustin,M.L., Erickson,H.P. and Springer,T.A. (1990) The arrangement of the immunoglobulin-like domains of ICAM-1 and the binding sites for LFA-1 and rhinovirus. *Cell*, **61**, 243–254.

Stoeckli,E.T. and Landmesser,L.T. (1995) Axonin-1, Nr-CAM, and Ng-CAM play different roles in the *in vivo* guidance of chick commissural neurons. *Neuron*, **14**, 1165–1179.

Stoeckli,E.T., Kuhn,T.B., Duc,C.O., Ruegg,M.A. and Sonderegger,P. (1991) The axonally secreted protein axonin-1 is a potent substratum for neurite growth. *J. Cell Biol.*, **112**, 449–455.

Stoeckli,E.T., Ziegler,U. and Sonderegger,P. (1993) Co-clustering and functional cooperation of NgCAM and axonin-1 in the substratum contact area of growth cones. *Soc. Neurosci. Abstr.*, **19**, 185.8.

Suter,D.M., Pollerberg,G.E., Buchstaller,A., Giger,R.J., Dreyer,W. and Sonderegger,P. (1995) Binding between the neural cell adhesion molecules axonin-1 and NrCAM/Bravo is involved in neuron–glia interaction. *J. Cell Biol.*, **131**, 1067–1081.

Traunecker,A., Oliveri,F. and Karjalainen,K. (1991a) Myeloma based expression system for production of large mammalian proteins. *Trends Biotechnol.*, **9**, 109–113.

Traunecker,A., Lanzavecchia,A. and Karjalainen,K. (1991b) Bispecific single chain molecules (Janusins) target cytotoxic lymphocytes on HIV infected cells. *EMBO J.*, **10**, 3655–3659.

Venstrom,K. and Reichardt,L. (1995) β_8 integrins mediate interactions of chick sensory neurons with laminin-1, collagen IV, and fibronectin. *Mol. Biol. Cell*, **6**, 419–431.

Vielmetter,J., Kayyem,J.F., Roman,J.M. and Dreyer,W.J. (1994) Neogenin, an avian cell surface protein expressed during terminal neuronal differentiation, is closely related to the human suppressor molecule deleted in colorectal cancer. *J. Cell Biol.*, **127**, 2009–2020.

Yoshihara,Y., Kawasaki,M., Tani,A., Tamada,A., Nagata,S., Kagamiyama,H. and Mori,K. (1994) BIG-1: a new TAG-1/F3-related member of the immunoglobulin superfamily with neurite outgrowth-promoting activity. *Neuron*, **13**, 415–426.

Yoshihara,Y., Kawasaki,M., Tamada,A., Nagata,S., Kagamiyama,H. and Mori,K. (1995) Overlapping and differential expression of BIG-2, BIG-1, TAG-1, and F3: four members of an axon-associated cell adhesion molecule subgroup of the immunoglobulin superfamily. *J. Neurobiol.*, **28**, 51–69.

Yuckenberg,P.D., Witney,F., Geisselsoder,J. and McClary,J. (1991) Site-directed *in vitro* mutagenesis using uracil-containing DNA and phagemid vectors. In McPherson,M.J. (ed.), *Directed Mutagenesis: A Practical Approach*. IRL Press, Oxford, UK, pp. 27–48.

Zuellig,R.A., Rader,C., Schroeder,A., Kalousek,M.B., von Bohlen und Halbach,F., Osterwalder,T., Inan,C., Stoeckli,E.T., Affolter,H.U., Fritz,A., Hafen,E. and Sonderegger,P. (1992) The axonally secreted cell adhesion molecule, axonin-1: primary structure, immunoglobulin- and fibronectin-type-III-like domains, and glycosyl-phosphatidyl-inositol anchorage. *Eur. J. Biochem.*, **204**, 453–463.

Received on August 10, 1995; revised on December 7, 1995